Supporting Information

A seed-like structured Mo@ZrS$_2$ catalyst on graphene nanosheets for boosting the performance of rechargeable Zn–air batteries

Ramasamy Santhosh kumar[a], Dilmurod Sayfiddinov[a], S Tamilarasi[a], Dong Jin Yoo[a,b*]

[a]Department of Energy Storage/Conversion Engineering of Graduate School (BK21 FOUR), Hydrogen and Fuel Cell Research Center, Jeonbuk National University, Jeonju, Jeollabuk-do, 54896 Republic of Korea

[b]Department of Life Science, Jeonbuk National University, Jeonju-si, Jeollabuk-do, 54896 Republic of Korea

Corresponding Email ID: djyoo@jbnu.ac.kr

Fax: +82-(0) 63-270-3909 Tel: +82-(0) 63-270- 3608

Material characterizations

A high-resolution electron transmission microscope, a field-emitting scanning electron microscope, an HR-TEM (JEM-ARM200F, JEOL), and the energy dispersive X-ray spectroscopy (EDS (SUPRA 40 VP; Carl Zeiss, Germany) were used to evaluate the morphology of all produced electrocatalysts. The X-ray diffraction (XRD) patterns of the produced electrocatalysts were analyzed using Cu K radiation ($\lambda = 0.154$ nm) and a PANalytical (X'PERT-PRO Powder) model. At the Centers over University-wide Research Facilities (CURF) of Jeonbuk National University (JBNU), Republic of Korea, the Raman spectrum of the catalysts was measured employing high-performance 3D mapping Imaging Raman spectroscopy with NANO PHOTON (RAMAN Touch), equipped with a 532 nm helium-neon laser. At the Korean Basic Science Institutes of Jeonju Center (KBSI), Republic of Korea, the chemical condition of the materials was investigated utilizing an X-ray photoelectron spectrometer (XPS; Axis-Nova, Kratos Inc.), and a Brunauer–Emmett–Teller (BET) Autosorb–iQ 2ST/MP physisorption analyzer was used to measure the surface area of the produced catalyst.

Electrochemical measurements

The ORR activities were carried out using A Gamry Reference 600 Potentiostat/Galvanostat/ZRA electrochemical workstation combined with a rotating ring-disk electrode (RRDE) rotator RRDE-3A (ALS Co., Japan). Platinum wire, Ag/AgCl, and RDE (diameter of 5 mm: 0.19625 cm^2) were used as the counter, reference, and working electrodes, respectively. 5 mg of the catalyst and 30 μL of 5% Nafion solution were dispersed in 1 mL of ethanol and DI water (3:1) solution and the mixture was sonicated for 60 minutes to create a homogenous ink. A similar procedure was used to obtain conventional Pt-C ink, and the results were compared with those obtained with a

commercial catalyst. After that, a rotating disk electrode was drop-coated with 15 μL of catalyst ink. N_2 or O_2 saturated 0.1 M KOH electrolyte was used for both cyclic voltammetry (CV: scan rate 50 mV s^{-1}) and linear-sweep voltammetry (LSV: 10 mV s^{-1}). LSV was conducted with a voltage window of 0.2−0.8 V vs. Ag/AgCl, and various RDE rotational speeds ranging from 400 to 2800 rpm. N_2 was purged in the 0.1 M KOH electrolyte for 30 minutes before each ORR measurement to maintain O_2 saturation during the experiments. Calculation for number of electron transfer during ORR, Plots of Koutecky–Levich (K–L) were employed to calculate the quantity of electrons moved at different potentials (J^{-1} vs $\omega^{-1/2}$)[1].

$$\frac{1}{J} = \frac{1}{J_L} + \frac{1}{J_K} = \frac{1}{B\omega^{1/2}} + \frac{1}{J_K} \qquad (1)$$

$$B = 0.62\, nF\, C_0\, D_0^{\frac{2}{3}}\, v^{-1/6} \qquad (2)$$

Where, J, J_L, and J_k are measured current density, diffusion-limiting current density and kinetic – limiting current density, respectively.

Zinc-air Battery Test

Carbon paper foam (~1 cm^2) was treated with ZrS_2/rGO and Mo@ZrS_2/rGO catalytic inks, each with a 3 mg cm^{-2} catalyst concentration. A zinc-air battery was constructed using an air cathode made of 0.25 mm thick zinc foil (Alfa Aesar, UK) and an electrolyte consisting of 6 M KOH and 0.2 M Zn $(CH_3COO)_2$. Utilizing a Gamry 600 electrochemical workstation, durability testing for long-term charge discharge cycles was investigated. By the same process, a ventilation cathode electrode made of Pt-C (20 weight percent) was also produced. Equations 1 and 2 were utilized to

determine the specific capacity (mA h g^{-1}) and power density (mW cm^{-2}) of zinc-air batteries employing Pt-C, ZrS$_2$/rGO, and Mo@ZrS$_2$/rGO as the ambient cathode.[2]

Power density (mW cm^{-2}) = Voltage × current density   (3)

Specific capacity (mA h g^{-1}) = current × service hours/weight of consumed Zn   (4)
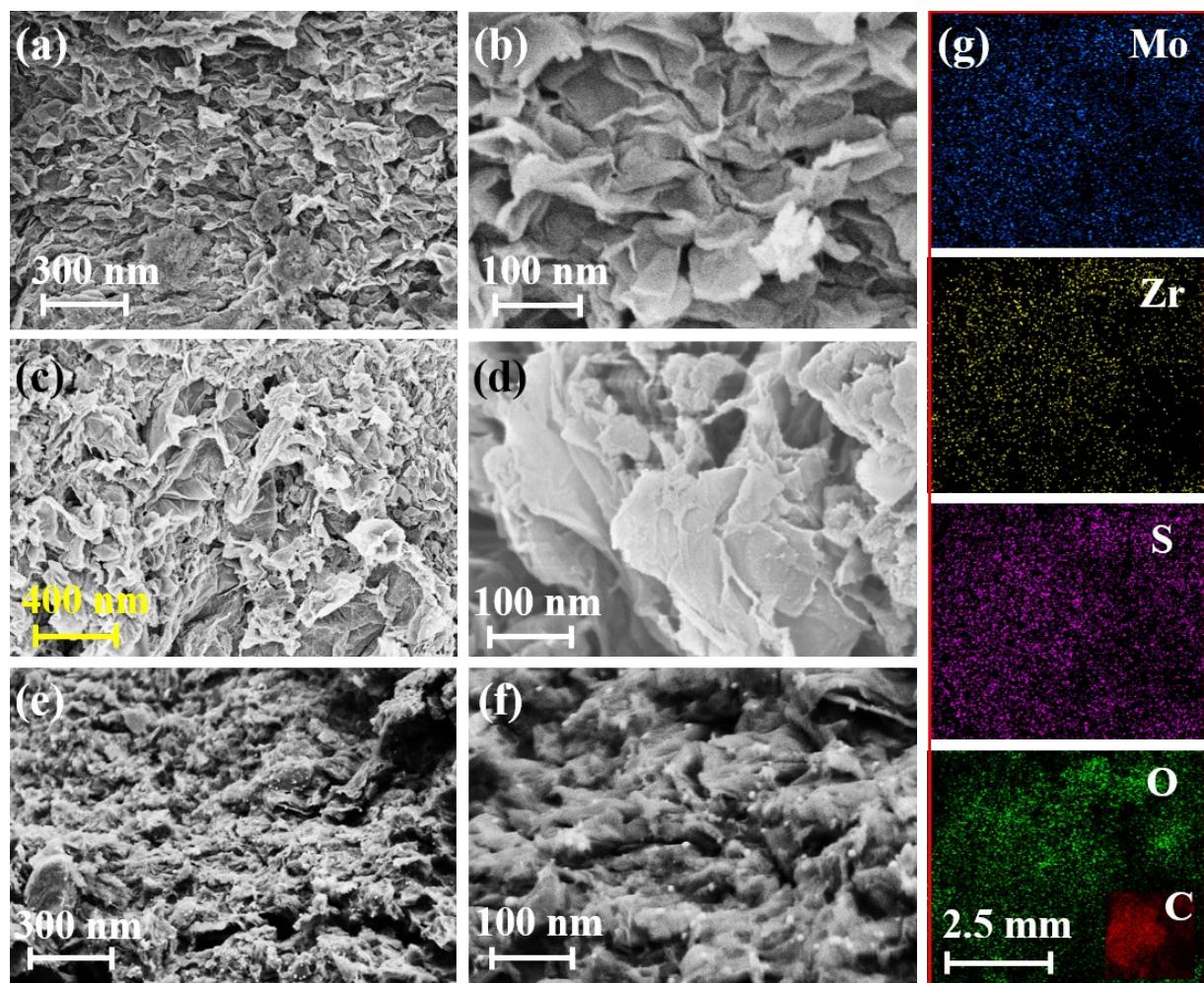
Fig. S1 SEM images of (a, b) graphene oxide nanosheets, (c, d) ZrS$_2$/rGO catalyst, (e, f) Mo@ZrS$_2$/rGO catalyst, and (g) EDS-elemental mapping of Mo@ZrS$_2$/rGO catalyst for following elements Mo, Zr, S, O, and C.
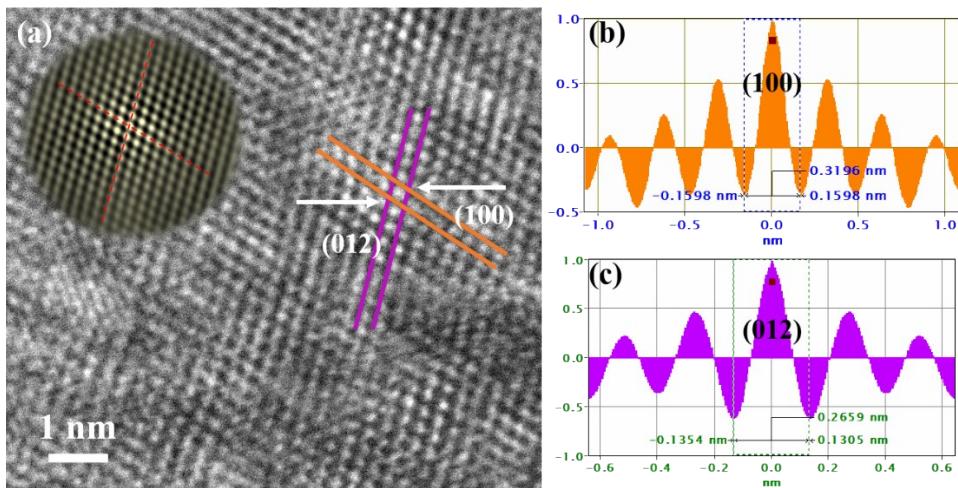
Fig. S2 (a) HR-TEM image and (b, c) corresponding lattice space line of Mo@ZrS$_2$/rGO catalyst.
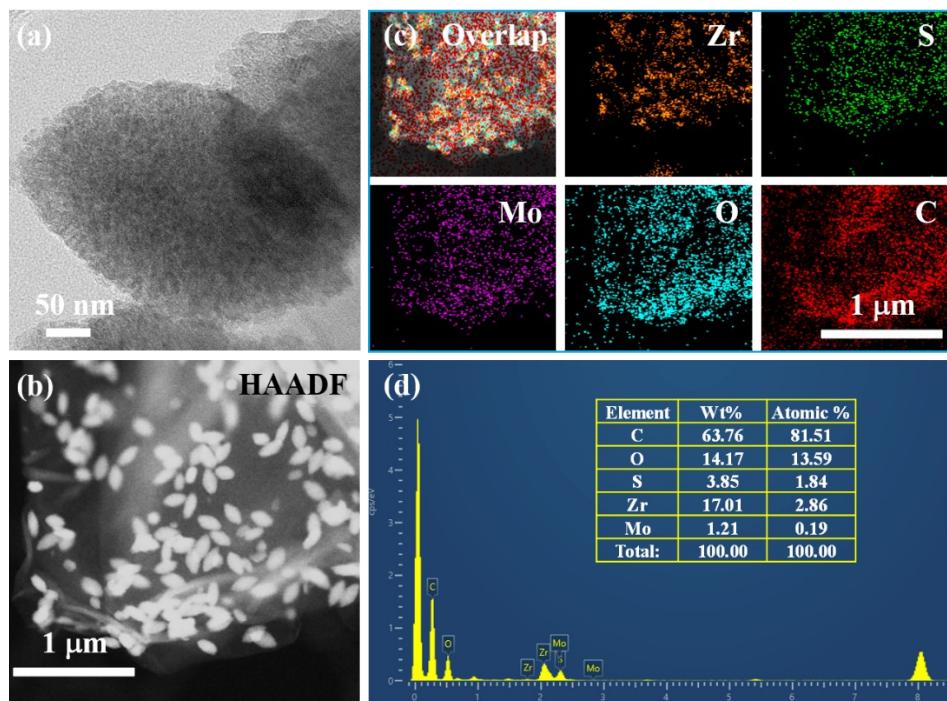

Fig. S3 TEM images of Mo@ZrS$_2$/rGO catalyst; (a, b) TEM and HAADF images, (d) TEM-EDS-elemental mapping for Mo, Zr, S, O, and C elements, (d) TEM-EDX spectrum (insert image; corresponding elemental percentages).
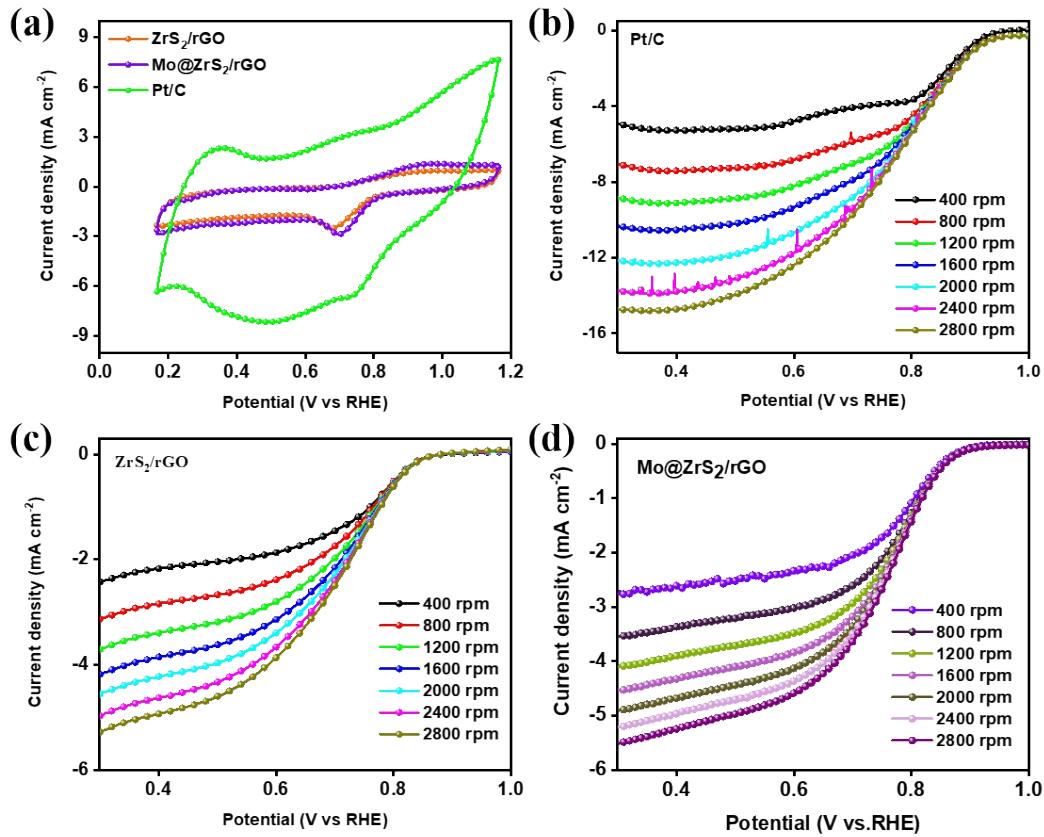
Fig. S4 ORR performance in 0.1 M KOH solution; (a) CV curves, (b, c, d) LSV curves of different rotating speeds for 400-2800 rpm for Pt-C, ZrS$_2$/rGO, and Mo@ZrS$_2$/rGO electrocatalysts.
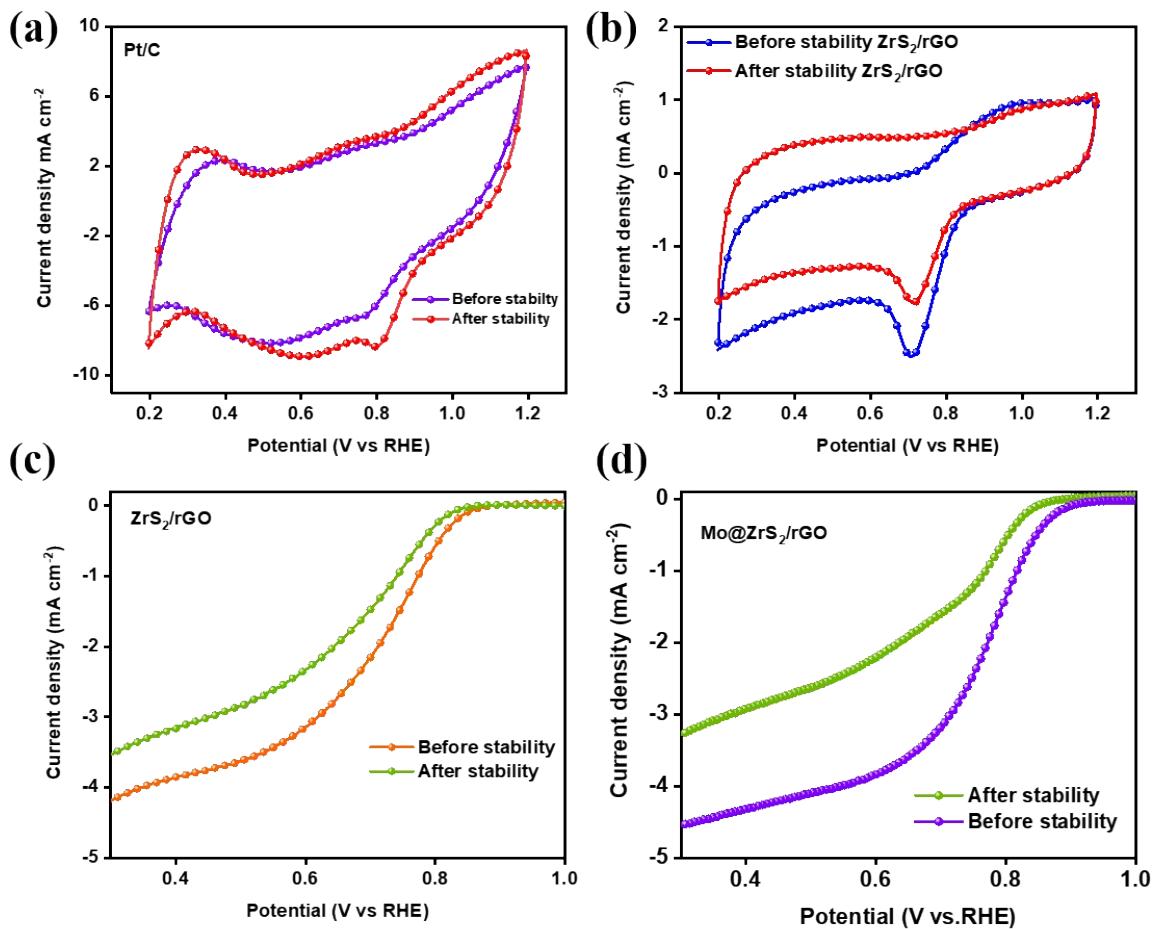
Fig. S5 ORR study after stability analysis; (a, b) before and after stability CV curves of Pt-C and ZrS$_2$/rGO electrocatalysts, (c, d) before and after stability LSV curves of ZrS$_2$/rGO and Mo@ZrS$_2$/rGO electrocatalysts, respectively.
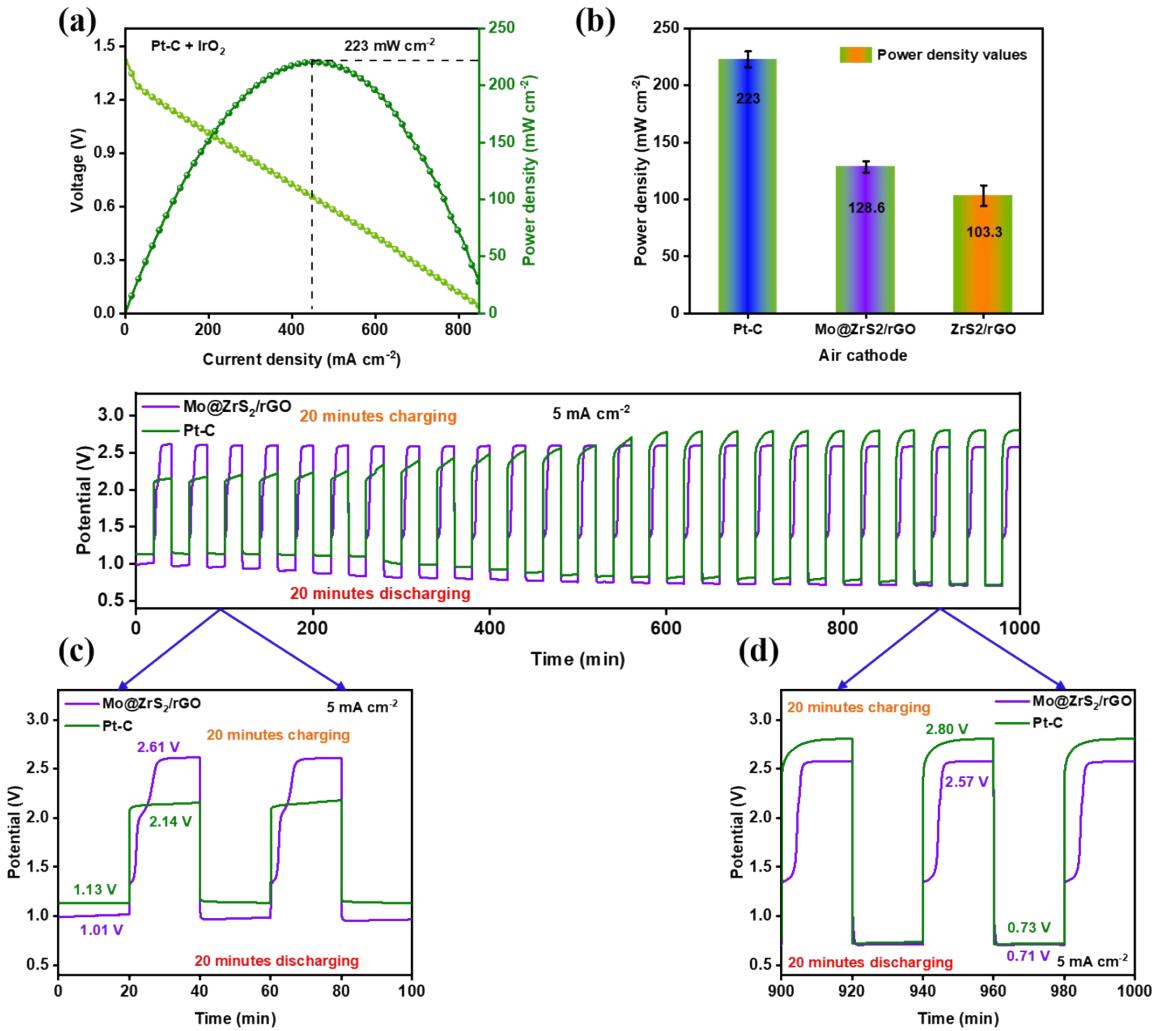
Fig. S6 (a) Power density curve of commercial Pt-C catalyst, (b) comparison of power density for commercial Pt-C, Mo@ZrS$_2$/rGO, and ZrS$_2$/rGO air cathode catalysts, respectively. (c, d) Zn-air batteries potential differences.
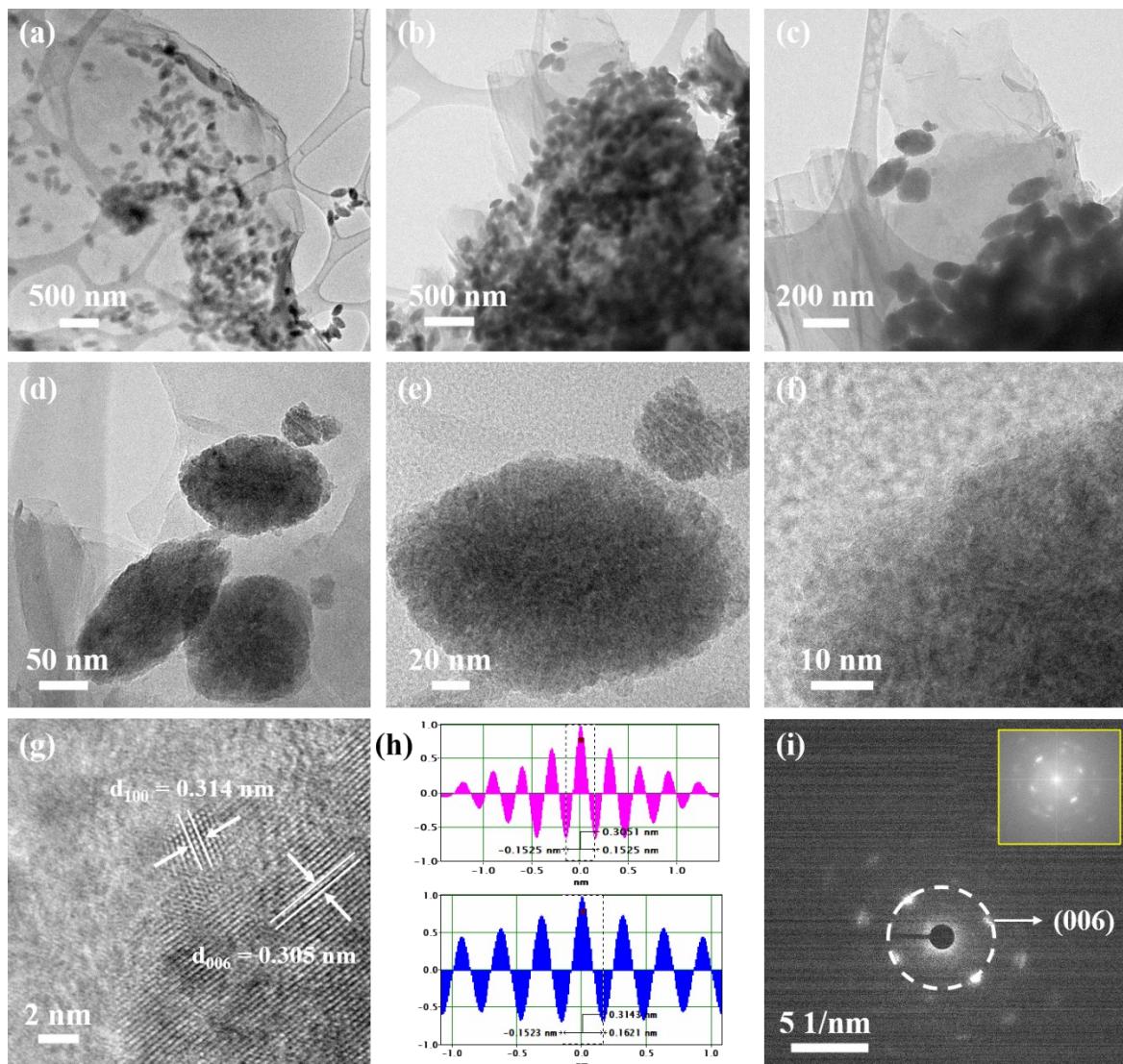
Fig. S7 post-morphology study for after ORR cyclic stability; (a-f) TEM images, (g) HR-TEM image, (h) lattice space crystal line, and (i) SAED pattern (insert image; FFT pattern) of Mo@ZrS$_2$/rGO catalyst.

Table S1. Comparison table of molybdenum based electrocatalysts for ORR (half wave potential) and Zn-air battery (power density) performances.

S.No	Catalysts	Half-wave potential (V)	Power density (mW cm^{-2})	Year of publication	References
1	Mo@ZrS$_2$/rGO	0.80	128.6	2024	This work
2	NiCoMoO$_4$@rGO	0.81	125.1	2023	[3]
3	Ni$_{0.5}$Mo$_{0.5}$OSe	0.88	166.7	2021	[4]
4	β-Mo$_2$C-Co	0.74	162	2023	[5]
5	O-Co$_{0.5}$Mo$_{0.5}$Se$_2$	0.83	120.2	2020	[6]
6	Co–Co$_6$Mo$_6$C$_2$@NPC	0.81	160.5	2023	[7]
7	NC@MoS$_2$@Co-Fe	0.73	97.1	2022	[8]
8	ZnCo-NCNT/Mo$_2$C-800	0.82	231.6	2023	[9]
9	Co(Zn$_{0.5}$)@MoS$_2$/CC	0.82	72.4	2023	[10]
10	Mo$_2$C/MoC/Co@CNTs	0.82	134	2024	[11]
11	FeCo-Mo$_{0.82}$N	0.78	149.7	2023	[12]
12	MoP@N, P-HCF	0.73	93.8	2021	[13]
13	P–MoO$_2$	0.78	104.6	2023	[14]
14	Meso-Mo$_2$C/C-0	0.81	115	2023	[15]
15	NiCo$_2$O$_4$/Mo$_2$C/CC	0.79	104	2021	[16]
16	NiFeMo@N-rGO-3	0.83	120	2021	[17]

References

1.   Y. Liang, Y. Li, H. Wang, J. Zhou, J. Wang, T. Regier and H. Dai, Co_3O_4 nanocrystals on graphene as a synergistic catalyst for oxygen reduction reaction, *Nature Materials*, 2011, **10**, 780-786.

2.   R. S. Kumar, S. Prabhakaran, S. Ramakrishnan, S. C. Karthikeyan, A. R. Kim, D. H. Kim and D. J. Yoo, Developing Outstanding Bifunctional Electrocatalysts for Rechargeable Zn-Air Batteries Using High-Purity Spinel-Type $ZnCo_2Se_4$ Nanoparticles, *Small*, 2023, **19**, 2207096.

3.   R. S. Kumar, P. Mannu, S. Prabhakaran, T. T. T. Nga, Y. Kim, D. H. Kim, J.-L. Chen, C.-L. Dong and D. J. Yoo, Trimetallic Oxide Electrocatalyst for Enhanced Redox Activity in Zinc–Air Batteries Evaluated by In Situ Analysis, *Advanced Science*, 2023, **10**, 2303525.

4.   J. Balamurugan, T. T. Nguyen, D. H. Kim, N. H. Kim and J. H. Lee, 3D nickel molybdenum oxyselenide ($Ni_{1-x}Mo_xOSe$) nanoarchitectures as advanced multifunctional catalyst for Zn-air batteries and water splitting, *Applied Catalysis B: Environmental*, 2021, **286**, 119909.

5.   W. Liu, X. Dai, W. Guo, J. Tang, J. Feng, D. Zheng, R. Yin, Y. Wang, W. Que, F. Wu, W. Shi and X. Cao, Phase Engineering of Molybdenum Carbide–Cobalt Heterostructures for Long-Lasting Zn-Air Batteries, *ACS Applied Materials & Interfaces*, 2023, **15**, 41476-41482.

6.   S. Prabhakaran, J. Balamurugan, N. H. Kim and J. H. Lee, Hierarchical 3D Oxygenated Cobalt Molybdenum Selenide Nanosheets as Robust Trifunctional Catalyst for Water Splitting and Zinc–Air Batteries, *Small*, 2020, **16**, 2000797.

7.   Y. Li, H. Wang, H. An, X. Liu, S. Chen and X.-Z. Song, Nano bowl-like cobalt–cobalt molybdenum carbide coated by N,P co-doped carbon as an advanced bifunctional oxygen electrocatalyst for rechargeable Zn–air batteries, *Dalton Transactions*, 2023, **52**, 6254-6259.

8.   X. Shang, Q. Shen, Y. Xiong, Z. Jiang, C. Qin, X. Tian, X. Yang and Z.-J. Jiang, Effect of Co-Fe alloy nanoparticles on the surface electronic structure of molybdenum disulfide nanosheets and its application as a bifunctional catalyst for rechargeable zinc air battery, *Journal of Alloys and Compounds*, 2022, **916**, 165482.

9. F. Li, J. Niu, Y. Liu, T. Qin, D. Zhao, Q. Zhao and X. Liu, One-dimensional hierarchical ZnCo-NCNT/Mo_2C nanostructure as a high-efficiency bifunctional catalyst for rechargeable Zn-air batteries, *Journal of Power Sources*, 2023, **553**, 232310.

10. X. Dong, J. Zhang, W. Shi, B. Wu, G. Wang, J. Chen and R. Wang, Heterointerfacial Cobalt/Zinc Sulfides on Molybdenum Disulfide Coated Carbon Cloth as Self-Supporting Electrode for Flexible Metal-Air Batteries, *ChemCatChem*, 2023, **15**, e202201472.

11. C. Xu, J. Zuo, J. Wang and Z. Chen, Hierarchically structured $Mo_{1-2}C$/Co-encased carbon nanotubes with multi-component synergy as bifunctional oxygen electrocatalyst for rechargeable Zn-air battery, *Journal of Power Sources*, 2024, **595**, 234063.

12. W. Liu, X. Niu, J. Feng, R. Yin, S. Ma, W. Que, J. Dai, J. Tang, F. Wu, W. Shi, X. Liu and X. Cao, Tunable Heterogeneous FeCo Alloy-$Mo_{0.82}N$ Bifunctional Electrocatalysts for Temperature-Adapted Zn–Air Batteries, *ACS Applied Materials & Interfaces*, 2023, **15**, 15344-15352.

13. M. He, C. Shu, R. Zheng, M. Li, Z. Ran, Y. Yan, D. Du, L. Ren and J. Long, Interfacial interaction between molybdenum phosphide and N, P co-doped hollow carbon fibers boosting the oxygen electrode reactions in zinc-air batteries, *Electrochimica Acta*, 2021, **395**, 139211.

14. X. Cui, Y. Tao, X. Xu and G. Yang, P-doping optimized d-band center position in MoO_2 with enhanced oxygen reduction reaction and oxygen evolution reaction activities for rechargeable Zn-air battery, *Journal of Power Sources*, 2023, **557**, 232519.

15. J.-Y. Zhang, C. Xia, Y. Su, L. Zu, Z. Zhao, P. Li, Z. Lv, J. Wang, B. Mei, K. Lan, T. Zhao, P. Zhang, W. Chen, S. Zaman, Y. Liu, L. Peng, B. Y. Xia, A. Elzatahry, W. Li and D. Zhao, Boosted Oxygen Kinetics of Hierarchically Mesoporous Mo_2C/C for High-current-density Zn–air Battery, *Small*, 2023, **n/a**, 2307378.

16. C. Xu, Q. Wang, S. Zhao and S. Wang, $NiCo_2O_4$ nanoneedle/Mo_2C-coated carbon cloth as efficient catalyst for water splitting and metal-air battery, *Synthetic Metals*, 2021, **280**, 116894.

17. W. Zeng, C. Wei, K. Zeng, X. Cao, M. H. Rümmeli and R. Yang, NiFeMo Nanoparticles Encapsulated within Nitrogen-Doped Reduced Graphene Oxide as Bifunctional Electrocatalysts for Zinc-Air Batteries, *ChemElectroChem*, 2021, **8**, 524-531.